



ORIGINAL ARTICLE

# Self nanoemulsifying drug delivery system of stabilized ellagic acid–phospholipid complex with improved dissolution and permeability



Amelia M. Avachat <sup>\*</sup>, Vijay G. Patel <sup>1</sup>

Department of Pharmaceutics, Sinhgad Technical Education Society's Post Graduate Research Centre, Sinhgad College of Pharmacy, Vadgaon (Bk.), Pune 411041, India

Received 6 August 2014; accepted 11 November 2014  
Available online 20 November 2014

## KEYWORDS

Ellagic acid;  
Self nanoemulsifying drug delivery system;  
Ellagic acid–phospholipid complex;  
*Ex vivo* permeability studies;  
Food effect

**Abstract** Ellagic acid (EA), a plant polyphenol known for its wide-range of health benefits has limited use due to its low oral bioavailability. In this study, a new self-nanoemulsifying drug delivery system (SNEDDS), based on the phospholipid complex technique, was developed to improve the oral bioavailability of ellagic acid. Ellagic acid–phospholipid complex was prepared by an anti-solvent method and characterized. Enhanced lipophilicity after the formation of ellagic acid–phospholipid complex was verified through solubility studies.

Preliminary screening was carried out to select oil, surfactant and co-surfactant. Ternary phase diagrams were constructed to identify the area of nanoemulsification. Formulations were optimized on the basis of globule size, cloud point and robustness to dilution. The optimized SNEDDS of ellagic acid–phospholipid complex showed mean globule size of  $106 \pm 0.198$  nm and cloud point at 83–85 °C.

The *in vitro* drug release from SNEDDS was found to be higher compared to EA suspension and complex, while *ex vivo* studies showed increased permeation from SNEDDS compared to EA suspension. Moreover, SNEDDS overcome the food effect which was shown by EA suspension. Thus, SNEDDS were found to be influential in improving the release performance of EA, indicating their potential to improve the oral bioavailability of EA.

© 2014 The Authors. Production and hosting by Elsevier B.V. on behalf of King Saud University. This is an open access article under the CC BY-NC-ND license (<http://creativecommons.org/licenses/by-nc-nd/3.0/>).

<sup>\*</sup> Corresponding author. Tel./fax: +91 020 24354720, mobile: +91 9822456636.

E-mail addresses: [prof\\_avachat@yahoo.com](mailto:prof_avachat@yahoo.com) (A.M. Avachat), [vijay.patel867@gmail.com](mailto:vijay.patel867@gmail.com) (V.G. Patel).

<sup>1</sup> Mobile: +91 9860014690.

Peer review under responsibility of King Saud University.



Production and hosting by Elsevier

## 1. Introduction

Over the past few decades, phytoconstituents, have infused a great interest and have developed more prevalence in the pharmaceutical industry and academia alike throughout the world as safer and effective alternative to synthetic drugs. Despite the promising effectiveness and safety of phytoconstituents, poor oral absorption due to their low aqueous solubility, rapid

metabolism and poor membrane permeability has led to plasma drug concentration below MEC resulting in poor bioavailability and less or no therapeutic effect which has ultimately limited their clinical use.

Ellagic acid (EA), (2,3,7,8-tetrahydroxy[1]benzopyran [5,4,3cde][1]benzopyran-5,10-dione), a dilactone of hexahydroxydiphenic acid is a polyphenolic flavonoid found in many dietary plant foods such as walnuts, pomegranates, strawberries, blackberries, cranberries, pecans and raspberries (Häkkinen et al., 2000). It has been reported that EA has many beneficial properties that help in the treatment of several oxidation-linked chronic diseases (Landete, 2011; Li et al., 2013; Vattem and Shetty, 2005) such as cardiovascular disease (Larrosa et al., 2010), prostate cancer (Bell and Hawthorne, 2008), neurodegenerative diseases (Porat et al., 2006) and breast cancer (Wang et al., 2012).

EA, an yellow ochre crystalline powder having melting point of more than 300 °C and a molecular weight of 302.02 Da, has poor solubility in water (~9.7 µg/ml) and methanol (~671 µg/ml) but is soluble in *N*-methyl pyrrolidone (NMP), pyridine, polyethylene glycol (400) and triethanolamine (Bala et al., 2006). Despite having several beneficial health effects, EA has limited potential for therapeutic use due to poor absorption because of low aqueous solubility (Lei et al., 2003), extensive metabolic transformation (Seeram et al., 2004) and rapid elimination leading to ineffective drug plasma concentration.

Several techniques have been suggested to conquer this oral bioavailability challenge of EA, including biodegradable *in situ* gelling systems, liposomes, incorporation of EA in self-assembled peptide microtubes and cellulose ester solid dispersions of EA (Sharma et al., 2007; Carballo et al., 2010; Barnaby et al., 2012; Li et al., 2013).

Recently, lipid based formulations have emerged as one of the best and effective solution to deliver poorly soluble drugs, among which, the self-nanoemulsifying drug delivery systems (SNEDDS) have proved to be a promising technology to enhance oral systemic bioavailability of poorly water soluble drugs or phytoconstituents (Villar et al., 2012; Singh et al., 2010; Hong et al., 2006).

SNEDDS are isotropic mixtures of active drug, oils, surfactants and usually one or more hydrophilic co-solvents or co-emulsifiers that on contact with aqueous medium upon mild agitation, form fine oil in water nanoemulsions of droplet sizes ranging from 20 to 200 nm (Mou et al., 2008; Porter et al., 2008). Thus small oil droplets of resulting nanoemulsions dispersed in the gastrointestinal fluids provide a large interfacial area for absorption enhancing the activity and minimizing the irritation due to contact of drug in the gut wall (Setthacheewakul et al. 2010).

It has also been observed that certain drug molecules are not stable in lipid system which necessitates the presence of antioxidants or chelating agents for enhancing their stability. Thus SNEDDS containing antioxidants or chelating agents provides formulation with improved bioavailability as well as adequate stability.

Several studies have shown that complexing polyphenolic compounds with phospholipids (PL) have improved their liposolubility as well as aqueous solubility and thus its therapeutic efficacy (Pathan and Bhandari, 2011; Shyam et al., 2012; Singh et al., 2012; Cao et al., 2012; Semalty et al., 2010; Khan et al., 2013). Such technique has also facilitated the incorporation of

large amount of low liposoluble compounds in lipid system (Zhang et al., 2011). Apart from improving liposolubility of polyphenolic compounds after complexation, PL themselves have a hepatoprotective, antilipemic and anti-atherogenic effects (Khan et al., 2013).

Thus, the purpose of this study was to develop and evaluate a novel SNEDDS formulation of ellagic acid–phospholipid complex (EAPL complex) stabilized by the presence of antioxidant.

## 2. Materials and methods

### 2.1. Materials

EA was purchased from Yucca Enterprises Pvt. Ltd, Mumbai, India. Capmul MCM C8, and captex 500 were gifted by Abitec Corp., USA. Capryol 90, labrafil M 2125 CS, labrafil M 2130 CS, labrafac CC, labrasol, lauroglycol FCC, transcutool P were kindly gifted by Gattefosse, France. Oleic acid, tween 80, tween 20, span 20, propylene glycol, PEG 400 and PEG 200 were purchased from Loba Chemie Pvt. Ltd., Mumbai. Cremophor RH 40 was a gift from BASF, Germany.

### 2.2. Preparation of EAPL complex by anti-solvent method

EAPL complex was prepared with EA and soy lecithin at a molar mass ratio of 1:1 by a slightly modified method from earlier reported method by Venkatesh et al. (2009). EA and soy lecithin were placed in 100 mL round bottom flask and mixed properly. Then to this mixture 50 mL of methanol was added. The mixture was refluxed at a temperature not exceeding 60 °C for 2 h with continuous stirring. Resultant solution was evaporated to 5–8 mL and 20 mL of *n*-hexane was added to it with continuous stirring. EAPL complex was precipitated, which was filtered and dried under vacuum. Resultant complex was collected and stored in a glass bottle at room temperature (Kuntal et al., 2007).

### 2.3. Characterization of EAPL complex

#### 2.3.1. Determination of EA content in EAPL complex

Content of EA in the complex was determined spectrophotometrically. Approximately 10 mg of the complex was dissolved in 1 mL of methanol in a 10 mL volumetric flask and the volume was adjusted to 10 mL. A portion of the sample was adequately diluted and analysed at 255 nm to evaluate the concentration of EA in the complex. The experiments were carried out in triplicate.

#### 2.3.2. Thin layer chromatography (TLC)

EAPL complex, pure EA and physical mixture of EA and PL were separately dissolved in ethyl acetate, spotted on Silica Gel 60 F254 pre-coated TLC plates and chromatogram was developed in a chromatographic chamber using chloroform: methanol (70:30) as solvent system at room temperature. After development of chromatogram, plates were exposed to iodine fumes and scanned using ultra violet fluorescence analysis cabinet (Biomedica Oswal Scientifics, Pune, India) and the  $R_f$  values of the spots were calculated and recorded.

### 2.3.3. Infra-red (IR) spectroscopy

The infrared spectra of EAPL complex, pure EA, pure PL and physical mixture of EA and PL were obtained by the KBr pellet method. Spectra were recorded in the region of  $4000\text{ cm}^{-1}$ – $400\text{ cm}^{-1}$ .

### 2.3.4. Differential scanning calorimetry (DSC)

The peak transition onset temperature of EAPL complex, pure EA and pure PL were determined and compared with the help of a Mettler DSC 30 S (Mettler Toledo, UK). Samples were sealed in the aluminium crimp cell and heated at the speed of  $10\text{ }^{\circ}\text{C}/\text{min}$  from  $30$  to  $400\text{ }^{\circ}\text{C}$  in nitrogen atmosphere ( $60\text{ ml}/\text{min}$ ).

### 2.3.5. Determination of solubility

To confirm the improved liposolubility of complex, solubility of EAPL complex and EA were determined in *n*-octanol, water,  $0.1\text{ N HCl}$ , acetate buffer pH 4.5, phosphate buffer pH 6.8. Excess amounts of EAPL complex and EA were added to each microtube containing  $1\text{ mL}$  of each solvent. Samples were kept at  $25\text{ }^{\circ}\text{C}$  with constant shaking on orbital shaker for  $48\text{ h}$  and then centrifuged (R-8C Laboratory Centrifuge, Remi Equipments Pvt. Ltd., Mumbai.) at  $6000\text{ rpm}$  for  $10\text{ min}$ . Afterwards, supernatants were removed, filtered to remove undissolved particles and suitably diluted with respective solvents. The concentration of EA in supernatants was quantified by UV spectroscopy at  $255\text{ nm}$ . Each experiment was carried out in triplicate.

## 2.4. Preparation of SNEDDS of EAPL complex

### 2.4.1. Screening of oil phase/surfactants/co-surfactants

Solubility of EAPL complex in different oils, surfactants and co-surfactants were determined in similar manner as mentioned above. Screening of oil phase was made on the basis of solubilization potential of oil phase for drug under investigation. An excess amount of EAPL complex was added to each microtube containing  $1\text{ mL}$  of each vehicle. The concentration of EAPL complex in supernatants was quantified by UV spectroscopy at  $255\text{ nm}$  as discussed in Section 2.3.4. Each experiment was carried out in triplicate.

Surfactants were screened on the basis of their emulsifying ability (Date and Nagarsenker, 2007). Each surfactant was screened against selected oil phase for its ease of formation of emulsion and percent transmittance. Briefly, selected oil phase and each surfactant in  $1:1$  ratio were mixed in capped vials followed by dilution with equal volume of distilled water to yield fine emulsion. The ease of formation of emulsions was observed by recording the number of volumetric flask inversions required to yield a uniform emulsion. The emulsions were allowed to stand for  $2\text{ h}$  and their percent transmittances were recorded by UV spectroscopy at  $638.2\text{ nm}$  using distilled water as blank (Date et al., 2007).

Relative efficacy of the co-surfactants to improve the nano-emulsification ability of the surfactants was assessed by the turbidimetric method (Date et al., 2007). Briefly, selected surfactants and each co-surfactant in  $1:1$  ratio were mixed in capped vials and this surfactant mixture were added to selected oil phase in  $2:1$  ratio and their percent transmittances were recorded by UV spectroscopy at  $638.2\text{ nm}$  as described above.

### 2.4.2. Selection of antioxidant for stabilization of EA

Three different antioxidants (butyl hydroxyl toluene (BHT), butyl hydroxyl anisole (BHA) and tocopherol) were screened for their effectiveness in preventing EA from oxidation. Each antioxidant was added to EA in the concentration of  $0.15\%$  w/v and to it selected oil was added in capped vials while one of the vials contained mixture of EA and oil without any antioxidant. All the samples were heated at  $70\text{ }^{\circ}\text{C}$  in  $10\text{ ml H}_2\text{O}_2$  for  $3\text{ h}$ . Infrared spectra of all samples were obtained by KBr pellet method to detect any interaction between antioxidant and EA to select the best suited antioxidant and also to confirm stability of EA in the samples by comparison with infrared spectra of pure EA.

### 2.4.3. Construction of the ternary phase diagram

Four SNEDDS systems were developed (Table 4). For each of these systems (A, B, C, D), ternary phase diagrams were constructed to identify self-nanoemulsifying region, where each apex of triangle represent  $100\%$  of oil, surfactant and co-surfactant respectively (Kommuru et al., 2001). By varying percentage of oil, surfactant and co-surfactant, twenty-seven formulations were prepared for the phase diagram of each system. Surfactant and co-surfactant were mixed in different volume ratios ( $1:1$ ,  $1:2$  and  $2:1$ ). For each phase diagram, oil and specific surfactant: co-surfactant ratio were mixed in ratios ranging from  $1:9$  to  $9:1$  (w/w) in nine different ratios viz;  $1:9$ ,  $2:8$ ,  $3:7$ ,  $4:6$ ,  $5:5$ ,  $6:4$ ,  $7:3$ ,  $8:2$ ,  $9:1$  (Villar et al., 2012). Only clear or slight bluish dispersions were considered in the nanoemulsion region of the diagram (Zhang et al., 2008; Elnaggar et al., 2009).

### 2.4.4. Preparation of EAPL complex SNEDDS

Fifteen formulations of the system D (Captex 500: Cremophor RH 40: PEG 400), which yield maximum self-nanoemulsifying area (Table 5), were selected for drug incorporation and further optimization. EAPL complex at constant weight of  $30\text{ mg}$  and antioxidant were dissolved in the surfactant/co-surfactant mixture ( $S_{\text{mix}}$ ) and gently shaken at  $37\text{ }^{\circ}\text{C}$  for  $5\text{ min}$ . The oily phase was then added and shaking was proceeded for  $20\text{ min}$  which was aided by sonication till a clear dispersion was obtained.

## 2.5. Optimization of SNEDDS formulations

Based on the former screening and ternary phase diagram study, the optimum drug loaded formulation was selected based on the following optimization criteria.

### 2.5.1. Robustness to dilution

Robustness of the selected formulations for dilution was evaluated by diluting all these formulations to  $50$ -,  $100$ -,  $250$  and  $1000$ -fold with distilled water. The diluted nanoemulsions were allowed to stand for  $2\text{ h}$  and monitored for any physical changes and their percent transmittances were recorded by UV spectroscopy at  $638.2\text{ nm}$  using distilled water as blank.

### 2.5.2. Globule size analysis

In this analysis, the mean globule size and PDI of the selected formulations after  $1000$ -fold dilution in distilled water was determined and compared. The globule size and PDI of the

EAPL complex SNEDDS were determined using Malvern Zetasizer (Nano ZS 90, UK).

### 2.5.3. Cloud point measurement

The cloud point value of fifteen SNEDDS formulations was determined and compared. Each formulation was diluted with water in the ratio of 1:100 and placed in a water bath with gradual increase ( $2^{\circ}/\text{min}$ ) in temperature (from 25 to  $80^{\circ}\text{C}$ ). Cloud point was measured as the temperature at which there was a sudden appearance of cloudiness as seen visually (Zhang et al., 2008).

## 2.6. Characterization of optimized EAPL complex SNEDDS formulation

### 2.6.1. Zeta potential (ZP) measurement

Charge on drug loaded droplet surface was determined using Zetasizer Beckman Coulter, Delsa TM Nano. Analysis time was kept for 60 s and average ZP, charge and mobility of optimized formulation of EAPL complex SNEDDS was determined. The zeta potential was measured after dilution of samples with distilled water at room temperature.

### 2.6.2. Centrifugation test

The EAPL complex SNEDDS sample was diluted 100 times with distilled water, centrifuged at 3500 rpm on centrifuge for 30 min and then examined visually for any phase separation.

## 2.7. Drug release studies

### 2.7.1. In vitro dissolution studies

*In vitro* dissolution tests were performed using a USP XXIV dissolution apparatus 1 (Lab India DS 8000) at  $37 \pm 0.5^{\circ}\text{C}$  and rotating speed of 50 rpm in 900 mL of dissolution media namely, 0.1 N HCl and phosphate buffer pH 6.8. SNEDDS formulation equivalent to 15 mg of EA (30 mg of EAPL complex) and EA suspension were filled in size “0” hard gelatin capsules which were then placed in the rotating basket. At predetermined intervals, an aliquot (5 ml) of the sample was collected and filtered through a membrane filter ( $0.45 \mu\text{m}$ ). The concentration of EA in the collected sample was analysed using UV spectroscopic method at 255 nm. An equivalent volume (5 ml) of fresh dissolution medium was added to compensate for any loss due to sampling.

### 2.7.2. In-vitro diffusion studies by dialysis bag method

Dialysis bag method were performed using USP XXIV dissolution apparatus 2 (Lab India DS 8000) at  $37 \pm 0.5^{\circ}\text{C}$  and rotating speed of 50 rpm in 900 mL of dissolution media namely, 0.1 N HCl and phosphate buffer pH 6.8. SNEDDS formulation and EA suspension in same amount as mentioned above were filled in  $6 \times 3$  cm dialysis bag (cut off 12,000 Da). Both the ends of bag were tightly tied to prevent any leakage and dialysis bag was fixed to the rotating paddle. At predetermined intervals, sampling and UV spectroscopic analysis of samples were performed in similar manner as mentioned above.

## 2.8. Effect of food on release profile of EA from unformulated EA and EAPL complex loaded SNEDDS

### 2.8.1. Preparation of modified biorelevant media, blank fed state simulated intestinal fluid (FeSSIF) and blank fasted state simulated intestinal fluid (FaSSIF)

Blank FeSSIF was prepared by dissolving 3.438 g of  $\text{NaH}_2\text{PO}_4$  and 6.186 g of NaCl in 500 ml of deionized water and pH was adjusted to 6.5 by NaOH pellets. Similarly, Blank FaSSIF was prepared by dissolving 8.65 g of acetic acid and 11.874 g of NaCl in 500 ml of deionized water and pH was adjusted by adding 4.04 NaOH pellets (Zoeller and Klein, 2007).

### 2.8.2. Dissolution studies

Release pattern of EA from unformulated EA and EAPL complex loaded SNEDDS was studied using USPXXIII apparatus I (Lab India DS 8000) at  $37 \pm 0.5^{\circ}\text{C}$  with a rotating speed of 50 rpm in blank FeSSIF and FaSSIF separately so as to evaluate the effect of food on *in vitro* dissolution. During the study, 10 ml of the aliquot was removed at predetermined time intervals (10, 15, 30, 45 and 60 min) from the dissolution medium and replaced with fresh medium. The amount of EA released in the dissolution medium was determined UV spectrophotometrically at 255 nm.

## 2.9. Ex vivo permeability studies

For *ex-vivo* permeability study, stomach and small intestine of the previously sacrificed Male Sprague–Dawley rat were isolated and thoroughly washed with phosphate buffer saline (PBS) to remove the mucous and lumen contents. EAPL complex SNEDDS diluted separately with 0.1 N HCl and phosphate buffer pH 6.8 were filled in the stomach and intestine respectively. An equivalent amount of EA suspension in 0.1 N HCl and phosphate buffer pH 6.8 respectively were used for comparison. Both the ends of the tissues were tied properly

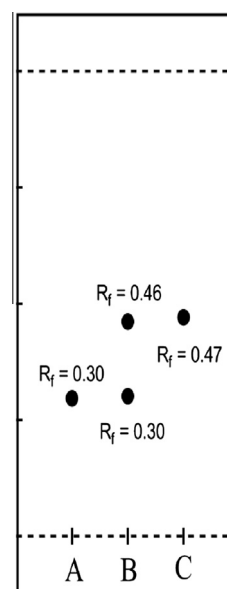


**Figure 1** TLC of (a) pure EA, (b) physical mixture of EA and PL and (c) EAPL complex.



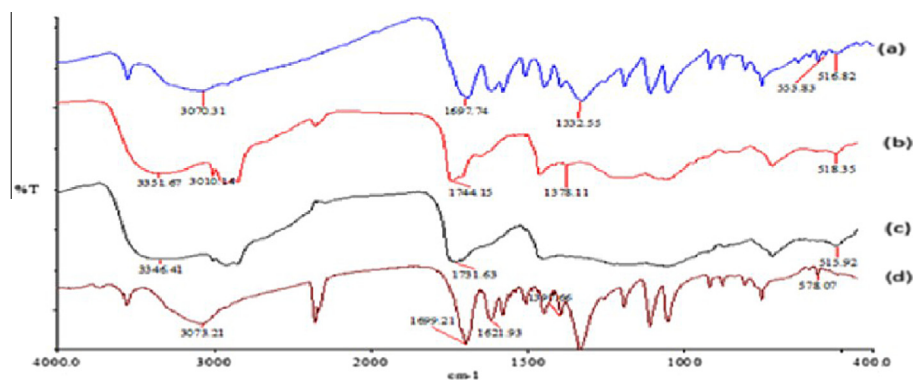


**Figure 2** IR spectra of (a) EA, (b) PL, (c) physical mixture of EA and PL and (d) EAPL complex.

to avoid any leakage and were put into beakers containing 40 ml of phosphate-buffered saline (pH 7.4) as the receptor phase with continuous bubbling of air under gentle stirring at  $37 \pm 2$  °C. Samples were withdrawn from the receptor phase at periodic time intervals and subjected to spectrophotometric analysis. All the experiments were performed in triplicate (Gupta et al., 2011).

### 3. Results and discussion

#### 3.1. Characterization of EAPL complex

##### 3.1.1. Content of EA in complex

The content of EA in the complex, as determined by UV spectroscopy, was 95.89% (w/w). This may be attributed to strong interaction between OH group of phenolic rings existing in the structure of the EA molecule and aqueous head of phospholipid molecule i.e. choline resulting in the formation of hydrogen bonding.

##### 3.1.2. Thin layer chromatography (TLC)

The TLC chromatograms of pure EA and the EAPL complex showed that pure EA has an  $R_f$  value of 0.309, whereas the complex has  $R_f$  value of 0.476 (Fig. 1). Pure EA showed smaller  $R_f$  value than that showed by complex which may be due to the fact that the more polar component tends to adhere more tightly to the plate whereas the less polar moiety tends to move along more freely with the mobile phase consisting of chloro-

form and methanol. Results confirmed the formation of EAPL complex as complex showed different  $R_f$  value than that showed by starting component i.e. pure EA.

##### 3.1.3. Infra-red spectra analysis

The IR spectra of EA, PL, physical mixture of EA and PL, EAPL complex are shown in Fig. 2. It is apparent that the physical mixture and the complex have distinct IR spectra. The characteristic absorption peak of EA at 1697.74 was found in IR spectrum of EA and physical mixture but was slightly shifted to 1621.93 in IR spectrum of complex. Moreover, broad peak in spectrum of EA at 3070.31 of O—H appeared broader and with more intensity in the case of complex indicating interactions between EA and PL. However, the characteristic absorption peak of PL was found in spectrums of both the complex and the physical mixture but appeared narrower may be due to the formation of complex. Furthermore, no new peaks were observed in the mixture and complex.

##### 3.1.4. Differential scanning calorimetry (DSC) analysis

DSC is a fast and reliable method to screen drug-excipient compatibility by providing maximum information about the possible interactions between them. In DSC, an interaction can be concluded by the elimination of endothermic peak(s), appearance of new peak(s), changes in peak shape and its onset, peak temperature/melting point and relative peak area or enthalpy. Fig. 3 shows the DSC thermograms of (a) EA,

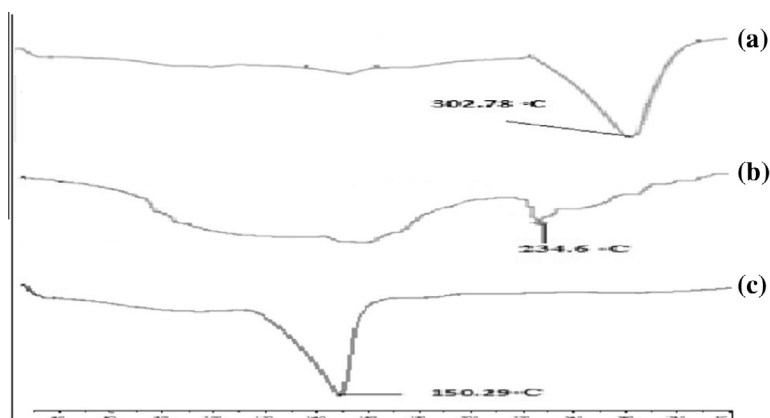


**Figure 3** DSC of (a) EA, (b) PL and (c) EAPL complex.

**Table 1** Solubility of ellagic acid and ellagic acid–phospholipid complex in water and *n*-octanol at 25 °C.

| Solvent           | Solubility of ellagic acid (mg/mL) | Solubility of ellagic acid phospholipid complex (mg/mL) |
|-------------------|------------------------------------|---|
| <i>n</i> -Octanol | 0.138 ± 0.04                       | 0.899 ± 0.02  |
| Water             | 0.0108 ± 0.06                      | 0.029 ± 0.03  |

(b) PL, and (c) EAPL complex. Thermogram of EA exhibits a single peak (302.78 °C) which is very sharp and it may be caused by the phase transition from solid state to liquid state or may have resulted from the decomposition of EA at such higher temperature. PL showed two different kinds of endothermic peaks. The first endothermic peak (140.9 °C) appears mild, indicating movements due to heating of choline structure of PL molecule. The second endothermic peak appears at 234.6 °C, which could be possibly due to the phase transition of PL molecule. DSC of EAPL complex showed that the endothermic peaks of both, EA and PL disappeared and the phase transition temperature appeared at 150.29 °C, which may be contributed to the formation of the complex and thus differed from that of EA and PL. It was evident that the original peaks of EA and PL disappeared from the thermogram of complex and the phase transition temperature was lower than that of EA. In this case, after combination of EA and polar parts of PL molecule i.e. choline, the hydrocarbon chain in PL may have twisted and wrapped the choline bound portion of PL molecule, causing the sequential energy to decrease in phosphatidyl portion, which may have resulted in the

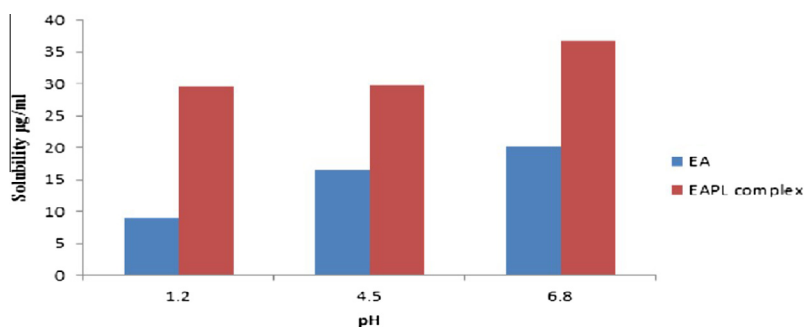
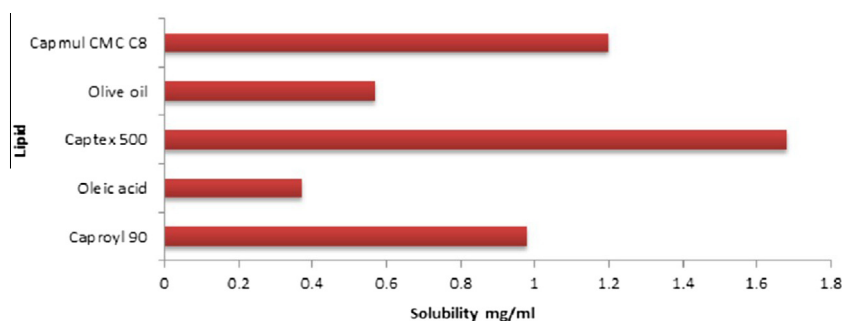
disappearance of the endothermic peak of PL and decline of the melting point i.e. phase transition temperature.

### 3.1.5. Determination of solubility

Compared to EA, EAPL complex exhibited much higher solubility in *n*-octanol and water, around 6 times and 3 times respectively (Table 1). Results confirmed that solubility of EA was enhanced complexing it with PL which may be attributed to the amphipathic nature of phospholipids having considerable solubility in both, aqueous and oily media. As pH of the aqueous phase has considerable influence on the phase behaviour of spontaneously emulsifying systems, therefore enhancement of solubility of EA after complexation in all pH ranges likely to be encountered was important. Solubility of EA increased with an increase in pH. Moreover EAPL complex also showed increase in its solubility with pH but was higher at all pH conditions compared to EA as shown in Fig 4. So it confirms the hypothesis that complexation is required to increase its lipid and aqueous solubility before its incorporation into SNEDDS.

### 3.2. Screening of oil phase/surfactant/co-surfactant

Solubility studies were performed for the selection of oil phase in order to determine individual solubilization capacity of each oil phase for drug under investigation as solubilizing capacity of an oily phase is an important consideration regarding oil phase selection (Pouton and Porter, 2008). Also in self-nanoemulsifying formulation to achieve optimum drug loading identification of the suitable oil, surfactant/co-surfactant having maximal solubilizing potential for drug under investigation

**Figure 4** Solubility of EA and EAPL complex at different pH conditions.**Figure 5** Solubility of EAPL complex in various oils.

is very important (Pouton, 1997, 2000). The solubility of the drug was tested in four different oily phases (capmul CMC C8, olive oil, captex 500, oleic acid, caproyl 90) that are frequently used in developing self-emulsifying formulation (Chen, 2008). Solubility of EAPL complex in various oily phases, surfactants and co-surfactants solutions is presented in Figs. 5–7, respectively. Solubility studies (Fig. 5) clearly indicated that amongst the various oil phases that were screened, captex 500 was found to solubilize maximum amount of EAPL complex  $1.680 \pm 0.087$  mg/mL followed by caproyl 90 and olive oil  $0.987 \pm 0.139$  mg/mL and  $0.570 \pm 0.012$  mg/mL, respectively. The higher solubility of EAPL complex in medium chain glycerides (captex 500, capmul MCM C8 and caproyl 90) than long chain glycerides may have arisen from the higher ester bond content per gram of the medium chain glycerides. Therefore in order to achieve ideal drug loading and to avoid precipitation of the drug on dilution in the gut lumen *in vivo*, captex 500 was selected for further study as it had maximum solubilizing capacity for EAPL complex (Pouton, 2006).

Non-ionic surfactants are generally considered less toxic and usually accepted for oral ingestion than ionic surfactants (Pouton et al., 2008). A right combination of low and high HLB surfactant is essential for the formation of a stable nano-emulsion, in the development of a self-emulsifying formulation (Craig et al., 1995; Pouton, 2000). In this study, eight different hydrophilic and hydrophobic non-ionic surfactants were utilized, amongst which few surfactants (tween 80, labrasol and cremophor RH 40) are reported to possess bioactive effects. These include inhibitory effects on p-gp and CYP enzymes such as that of cremophor RH40 (Chen, 2008), effects on tight junction such as by labrasol (Hu et al., 2001) and lymphotropic character such as shown by tween 80 (Elnaggar et al., 2009).

**Table 2** Emulsification efficiency with different surfactants and selected oils.

| Surfactant       | % Transmittance at 638.2 nm |
|------------------|-----------------------------|
| Lauroglycol      | 27.15                       |
| Labrafac WL 1349 | 48.44                       |
| Labrafil M 2125  | 0.49                        |
| Brij-35          | 93.45                       |
| Triton X-100     | 96.64                       |
| Tween 20         | 88.29                       |
| Tween 80         | 84.55                       |
| Cremophor RH 40  | 96.54                       |

The surfactants were evaluated for their ability to emulsify the selected oily phases. It has been reported that well formulated SNEDDS is dispersed within seconds under gentle stirring conditions (Pouton et al., 2008). Transmittance values of different mixtures are demonstrated in Table 2. Emulsification studies clearly distinguished the ability of various surfactants to emulsify captex 500. These studies indicated that cremophor RH 40, triton X-100 and brij-35 had a very good ability to emulsify captex 500 followed by tween 20 and tween 80, whereas, lauroglycol, labrafac WL 1349, labrafil M 2125 were found to be poor emulsifiers for captex 500. Good emulsifying ability of cremophor RH 40, triton X-100 and brij 35 may be contributed to their same length of carbon chain (C8-C16) as that of selected oil phase. Even though, the HLB values of the surfactants used in the study were in the range of 1–16, there was a great dissimilarity in their emulsification ability. Obtained results are in line with those demonstrated by Malcolmson et al. (1998) and Warisnoicharoen et al. (2000) where they have concluded that microemulsification also

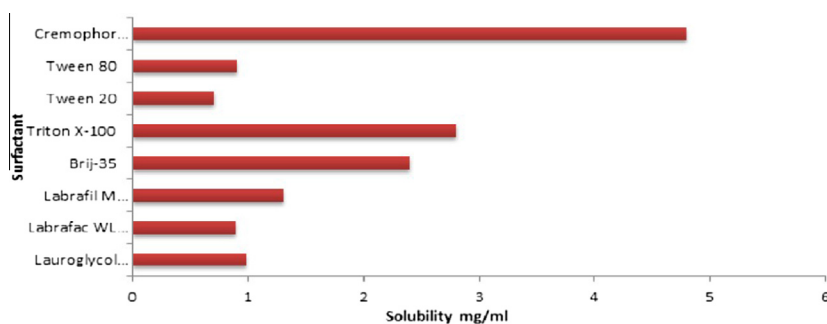


**Figure 6** Solubility of EAPL complex in various surfactants.

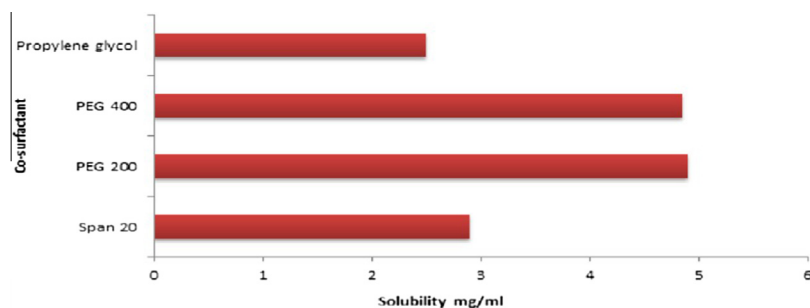


**Figure 7** Solubility of EAPL complex in various co-surfactants.

**Table 3** Emulsification efficiency with different co-surfactants and selected surfactants.

| Co-surfactant    | Cremophor RH 40<br>(% transmittance) | Triton X-100<br>(% transmittance) |
|------------------|--------------------------------------|-----------------------------------|
| Span 20          | 28.59                                | 39.12                             |
| PEG 200          | 98.25                                | 99.46                             |
| PEG 400          | 98.62                                | 99.88                             |
| Propylene glycol | 94.56                                | 95.81                             |

depends on the structure and chain length of the surfactant. As shown in Fig. 6, solubilizing capacity for drug under investigation of cremophor RH40 and triton X-100 was higher than that of the other surfactants and also both exhibited the highest emulsification efficiency with captex 500. Based on solubilization potential, emulsification ability and bioactive features, cremophor RH40 and triton X-100 were selected for further study.

Incorporation of a co-surfactant in the formulation containing surfactant was reported to improve dispersibility and drug absorption from the formulation (Porter et al., 2008). In consideration of current investigation, four co-surfactants, namely span 20, polyethylene glycol 400, polyethylene glycol 200 and propylene glycol were compared. The investigations clearly demonstrated the ability of various co-surfactants to improve the nanoemulsification of selected surfactant/s. As depicted in Table 3, captex 500 exhibited good emulsification with all co-surfactants, except span 20, with polyethylene glycol 400 showing maximum transmittance followed by polyethylene glycol 200. Moreover, results of solubility study demonstrated in Fig. 7 concluded higher solubility in polyethylene glycol 400 and 200 as compared to other co-surfactants which may be contributed to the fact that PEGs are miscible with both aqueous as well as organic solvents. Moreover, phenolic groups and lactone moiety in the structure of EA suggests higher chances of solubility in solvents with which it can form hydrogen bonds. Thus, hydrogen bonding might be playing a major role in solubilization of EA in PEG 400. Accordingly, PEG-400 and PEG-200, which gave higher transmittance values and solubility, were selected as co-surfactants for further investigations.

### 3.3. Screening of antioxidants

Due to the phenolic nature of EA which makes itself a powerful antioxidant, it gets oxidized in the presence of oil phase as

**Table 4** Components of four SNEDDS systems.

| System | Oil phase  | Surfactant      | Co-surfactant |
|--------|------------|-----------------|---------------|
| A      | Captex 500 | Triton X-100    | PEG 200       |
| B      | Captex 500 | Triton X-100    | PEG 400       |
| C      | Captex 500 | Cremophor RH 40 | PEG 200       |
| D      | Captex 500 | Cremophor RH 40 | PEG 400       |

confirmed by IR spectra of physical mixture of EA and captex 500. In SNEDDS formulation, oil phase is an essential component which necessitates addition of another antioxidant in formulation to prevent EA from being oxidized. Three oil soluble antioxidants were screened for their potential to prevent oxidation of EA in the presence of oil phase. From Fig. 8, it can be clearly seen that in the presence of tocopherol, many characteristic peaks of IR spectra of EA were retained even in the presence of oil phase (captex 500) while in case of BHT and BHA these peaks disappeared indicating that these antioxidants were not able to prevent oxidation of EA. Therefore it was concluded that tocopherol (0.15% w/v) was able to prevent oxidation of EA in the presence of oil phase and thus it was selected as antioxidant in the development of SNEDDS formulation (Solon et al., 2000; Festa et al., 2001).

### 3.4. Ternary phase diagram

Based on preliminary screening studies, ternary phase diagrams of four different (oil: surfactant: co-surfactant) system (Table 4) were constructed to identify self nanoemulsifying area of each system. The phase diagrams are depicted in Fig. 9. The shaded area in the triangle represents the region of self-nanoemulsion region in which the SNEDDS form fine oil in water emulsion under gentle agitation. Surfactant and co-surfactant are adsorbed at the interface, which reduces the interfacial energy and increases the mechanical barrier to coalescence leading to improved thermodynamic stability of the nanoemulsion formulation (Reiss, 1975). Additionally, co-surfactants by penetrating into the surfactant film and creating void space among surfactant molecules, increases the interfacial fluidity (Constantinides and Scalart, 1997). Wider region is a sign of better self-nanoemulsifying ability. In view of this fact, the wider nanoemulsification region of system D phase diagram (Fig. 9d) compared to that of the other system (A, B and C) showed better self nanoemulsification property of the former system. System D yielded nanoemulsion (globule

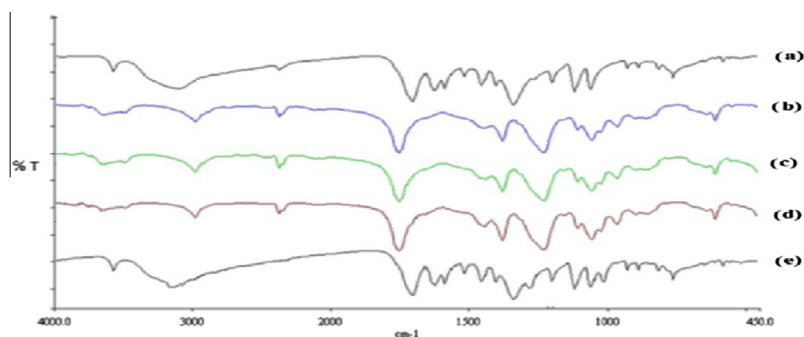


**Figure 8** Infrared spectra of (a) EA, (b) mixture (EA + captex 500), and (c) mixture in the presence of butylated hydroxyl toluene, (d) mixture in the presence of butylated hydroxyl anisole, (e) mixture in the presence of tocopherol.



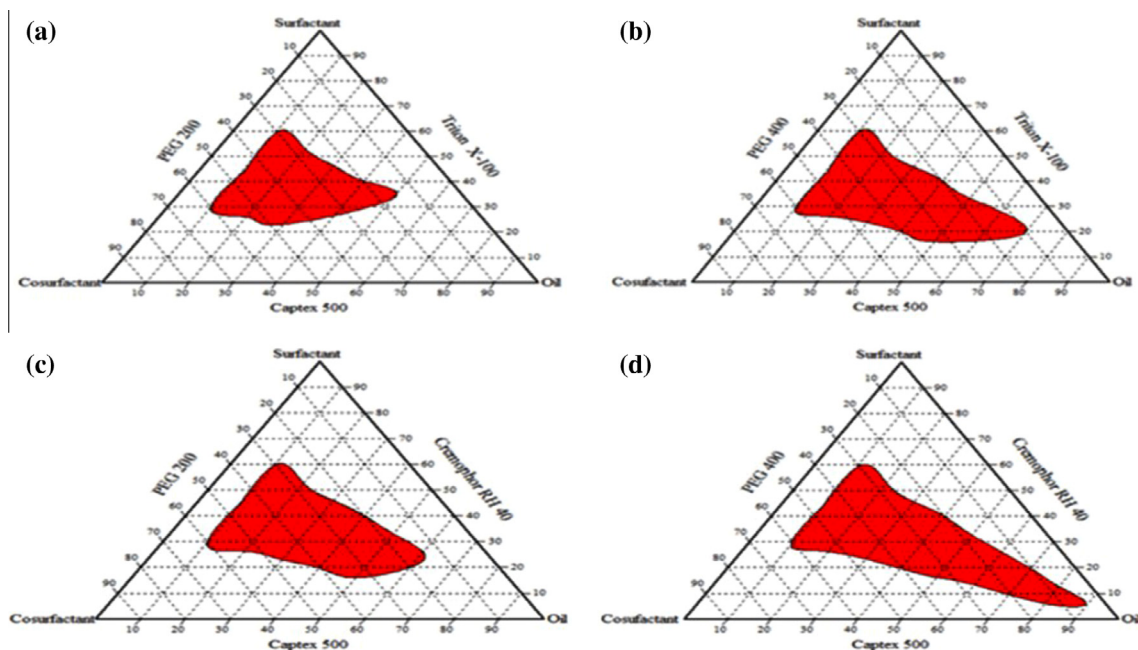


**Figure 9** Ternary phase diagrams of the selected systems dispersed in water at 25 °C. The shaded area represents self-nanoemulsion region. (a) captex 500: triton X-100: PEG 200 (b) captex 500: triton X-100: PEG 400 (c) captex 500: cremophor RH 40: PEG 200 (d) captex 500: cremophor RH 40: PEG 400.

size < 200 nm) containing as high as 80% oily phase composition. Nanoemulsions of globule size less than 150 nm were attained with up to 60% oil phase. However, mean globule size increased with increasing oil concentration and decreasing Smix concentration. This phenomenon could be attributed to the higher concentrations of the Smix required to produce fine and stable nanoemulsions due to the fact that smaller is the desired globule size, greater is the surface area and hence, greater amount of Smix required to stabilize the oil globules. Owing to wider nanoemulsion region and greater capacity for the incorporation of oily phase, system D was selected for further investigation.

### 3.5. Preparation of EAPL complex SNEDDS

EAPL complex (30 mg) was loaded in selected fifteen SNEDDS formulations. Composition of the fifteen formulations (F1–F15) is shown in Table 5.

### 3.6. Optimization of SNEDDS formulation

The best EAPL complex loaded formulation was selected among fifteen SNEDDS (F1–F15) based on the following tests.

#### 3.6.1. Robustness to dilution

SNEDDS formulations were subjected to different folds of dilution in order to mimic the *in vivo* conditions where the formulation would come across gradual dilution which may affect drug release profile and the drug may get precipitated at higher dilutions, which significantly retards its permeation or absorption (Constantinides, 1995). Hence, robustness to dilution was observed at 50, 100, 250 and 1000 fold dilution with distilled

water. All resulting dispersions showed no cloudiness, separation or precipitation, for 24 h, confirming their robustness to different dilution volumes of distilled water. Furthermore, it also points out to the probability of uniform *in vivo* drug release profile when the formulation encounters gradual dilution (Elnaggar et al., 2009).

#### 3.6.2. Globule size analysis

The droplet size of the emulsion is an important factor in self-emulsification performance as it determines the rate and extent of drug release, in addition to absorption (Shah et al., 1994; Gershanik and Benita, 1996). Smaller globule size is highly

**Table 5** Composition of SNEDDS formulations.

| Formulation no | Captex 500 (% v/v) | Cremophor RH 40 (% v/v) | PEG 400 (% v/v) | EAPL complex (mg/ml) | Tocopherol (mg/ml) |
|----------------|--------------------|-------------------------|-----------------|----------------------|--------------------|
| F1             | 10                 | 60                      | 30              | 30                   | 15                 |
| F2             | 20                 | 53                      | 26              | 30                   | 15                 |
| F3             | 30                 | 46                      | 23              | 30                   | 15                 |
| F4             | 40                 | 40                      | 20              | 30                   | 15                 |
| F5             | 50                 | 33                      | 16              | 30                   | 15                 |
| F6             | 60                 | 26                      | 13              | 30                   | 15                 |
| F7             | 70                 | 20                      | 10              | 30                   | 15                 |
| F8             | 80                 | 13                      | 06              | 30                   | 15                 |
| F9             | 90                 | 06                      | 03              | 30                   | 15                 |
| F10            | 30                 | 23                      | 46              | 30                   | 15                 |
| F11            | 40                 | 20                      | 40              | 30                   | 15                 |
| F12            | 50                 | 16                      | 33              | 30                   | 15                 |
| F13            | 60                 | 13                      | 26              | 30                   | 15                 |
| F14            | 30                 | 35                      | 35              | 30                   | 15                 |
| F15            | 40                 | 30                      | 30              | 30                   | 15                 |

**Table 6** Mean globule size, polydispersity index and cloud point of different SNEDDS formulations.

| Formulation no | Mean globule size (nm) | Polydispersity index | Cloud point (°C) |
|----------------|------------------------|----------------------|------------------|
| F1             | 269 ± 0.294            | 0.4892               | 75–77            |
| F2             | 139 ± 0.177            | 0.4128               | 71–73            |
| F3             | 284 ± 0.118            | 0.6538               | 78–79            |
| <b>F4</b>      | <b>106 ± 0.198</b>     | <b>0.3388</b>        | <b>83–85</b>     |
| F5             | 374 ± 0.203            | 0.3892               | 78–80            |
| F6             | 419 ± 0.271            | 0.7382               | 70–71            |
| F7             | 489 ± 0.382            | 0.4829               | 43–45            |
| F8             | 476 ± 0.109            | 0.6938               | 43–46            |
| F9             | 577 ± 0.392            | 0.8723               | 33–35            |
| F10            | 124 ± 0.145            | 0.6717               | 74–76            |
| F11            | 187 ± 0.157            | 0.1084               | 82–83            |
| F12            | 539 ± 0.348            | 0.5993               | 63–65            |
| F13            | 579 ± 0.293            | 0.4912               | 86–87            |
| F14            | 121 ± 0.231            | 0.5882               | 88–90            |
| F15            | 167 ± 0.118            | 0.3018               | 77–78            |

The values shown in bold represent most promising batches.

desirable, as it provides larger surface area for drug absorption. Results of globule size analysis are shown in Table 6. Six formulations (F2, F4, F10, F11, F14 and F15) showed globule size below 200 nm, amongst which F4 shows smallest globule size (106 ± 0.198) and lower PDI indicating narrow globule size distribution. The minimum globule size may have resulted due to minimum ratio of disperse phase to continuous phase.

### 3.6.3. Cloud point measurement

The cloud point is a crucial factor in SNEDDS particularly consisting of non-ionic surfactants as at temperature above cloud point formulation clarity turns into cloudiness. Even at

temperatures higher than the cloud point dehydration of polyethylene oxide moiety of the non-ionic surfactant may occur resulting in phase separation and there of affecting drug absorption (Elnaggar et al., 2009). Hence, to circumvent this occurrence of cloudiness and phase separation, the cloud point of the formulation should be over 37 °C. Many factors such as amount of each of the oils, surfactants and co-surfactants used, combination of excipients used, mixing ratio and drug hydrophobicity has a great influence on cloud point (Itoh et al., 2002; Zhang et al., 2008). All formulations showed cloud point at a very high temperature (37 °C is the base line), indicating stability at physiological temperature encountered in GIT, except F9 which exhibited cloudiness at 33–35 °C (Table 6).

### 3.7. Characterization of optimized SNEDDS formulation

#### 3.7.1. Zeta potential measurement

Zeta potential is a very important factor in characterizing SNEDDS formulation as it can identify the charge of oil globules in the emulsion (Gershanik and Benita, 2005). High zeta potential (negative or positive) indicates greater electrostatic repulsive forces between the globules which prevents the coalescence of nanoemulsion. On the other hand, decrease in such repulsive forces may lead to phase separation. The zeta potential of dispersion produced by EAPL complex SNEDDS following the 100 fold dilution with distilled water was found to be –13.31 mV as shown in Fig. 10, which may be due to higher concentration of surfactants in optimized EAPL complex SNEDDS, stabilizing the oil droplet resulting in more repulsive force between droplets. The negative value indicates that oil globules are negatively charged which may due to the presence of surfactants and/or co-surfactants. Moreover, SNEDDS showed conductivity of 0.1042 mS/cm (Fig. 10) which was higher than 0.50 mS/cm, indicating formation of o/w emulsion.

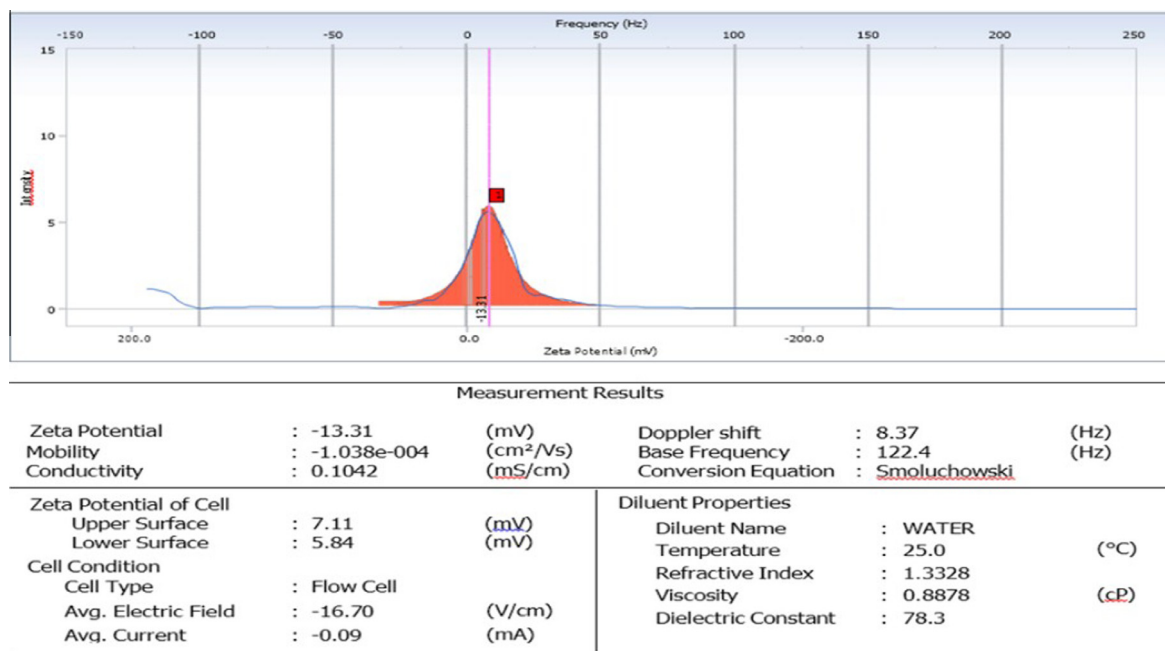


**Figure 10** Zeta potential of the SNEDDS formulation.

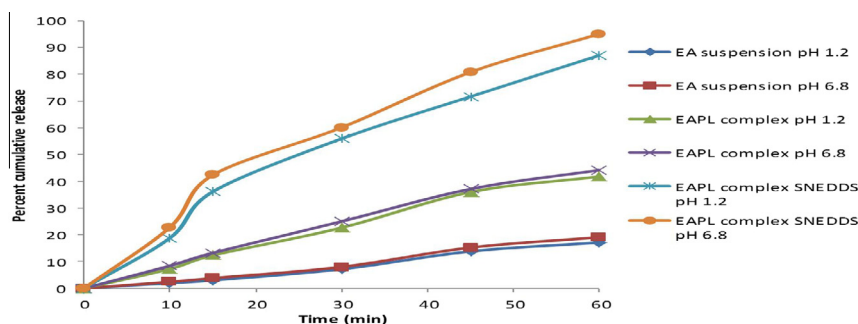


**Figure 11** Drug Release Profiles of EAPL complex SNEDDS, EAPL complex and EA suspension in 0.1 N HCl and phosphate buffer pH 6.8.

### 3.7.2. Centrifugation test

This test is usually used to determine the stability of the SNEDDS after nanoemulsion formation (Shafiq et al., 2007). Neither phase separation nor any precipitations were observed upon centrifugation of EAPL complex SNEDDS, indicating that a stable nanoemulsion is formed from EAPL complex SNEDDS.

### 3.8. Drug release studies

#### 3.8.1. In vitro dissolution profile

In the self-emulsifying systems, the free energy required to form an emulsion is very low, thereby allowing spontaneous formation of an interface between the oil droplets and water. It is suggested that the oil/surfactant/co-surfactant and water phases effectively swell, decrease the oil droplet size and eventually increase the release rate. *In-vitro* drug release studies were performed in 0.1 N HCl and pH 6.8 phosphate buffer. Release patterns (Fig. 11) reveal that EA release was significantly higher from EAPL complex SNEDDS (87.09%) as compared to that from EAPL complex and EA suspension which did not exceed 42% and 18% respectively after 60 min in HCl buffer. Similar results were obtained in the case of phosphate buffer (pH 6.8), where release from EAPL complex SNEDDS was about 95%, 44% and 19% respectively. It may be due to the fact that EAPL complex SNEDDS had resulted in spontaneous formation of a nanoemulsion with a small mean globule size, resulting in a faster rate of drug release into the aqueous phase than that of EA. Thus, this greater availability of dissolved EA from

the SNEDDS would lead to higher absorption and oral bio-availability. These results confirmed the role of SNEDDS formulation in improving EA solubilization and increased *in vitro* release.

#### 3.8.2. In-vitro diffusion profile by dialysis bag method

When SNEDDS comes in contact with aqueous medium in GIT, different forms of solubilized drug are formed including free molecular state, drug in nanoemulsion and drug in micellar solution. Under such situation to mimic *in vivo* dissolution condition, it becomes essential to separate free drug molecules from those entrapped in the nanoemulsion droplets or micelles. Therefore, conventional release testing is not completely adequate to this system so additionally dialysis bag method was carried out (Zhang et al., 2008). *In vitro* release patterns of EA from plain suspension and EAPL complex SNEDDS in HCl buffer (pH 1.2) and phosphate buffer (pH 6.8) are depicted in Fig. 12. The patterns reveal that release from EAPL complex SNEDDS was significantly higher than that from EA suspension. After 60 min, drug release from EAPL complex SNEDDS was about 79% compared to less than 15% from EA suspension in HCl buffer. Whereas in phosphate buffer pH 6.8 release from EAPL complex SNEDDS was about 95% and less than 15% from EA suspension. Results demonstrated that after formulating SNEDDS, the release profile of EA was significantly improved (6-fold) although the release was less from both EAPL complex SNEDDS and EA suspension in dialysis bag method compared to conventional dissolution method, which may be due to the restriction of the movement across the dialysis bag of

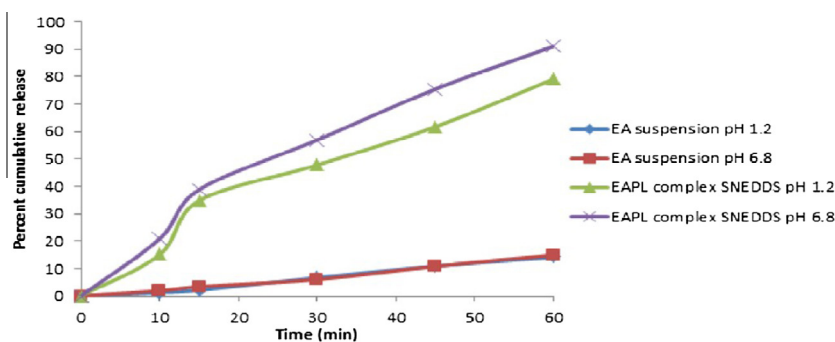


**Figure 12** *In vitro* drug release profiles of EAPL complex SNEDDS and EA suspension in HCl buffer pH 1.2 and phosphate buffer pH 6.8 by dialysis bag method.

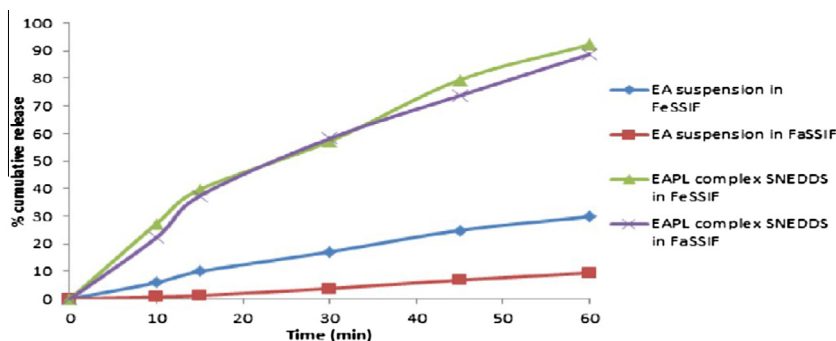


**Figure 13** *In-vitro* drug release profile of EAPL complex SNEDDS and EA suspension in FeSSIF and FaSSIF.

the separated free EA molecules from those entrapped in the nanoemulsion droplets. This proves the hypothesis that dialysis bag method mimics the *in vivo* dissolution precisely than that by conventional dissolution in *in vitro* evaluation of SNEDDS.

### 3.9. Effect of food on release profile of EA

It has been reported in the literature that drug formulated in SNEDDS circumvents the food effect w.r.t. its release. To prove this hypothesis dissolution of EA and formulated SNEDDS was carried out in modified biorelevant media, blank FeSSIF and FaSSIF to mimic *in vivo* conditions.

#### 3.9.1. Preparation of modified biorelevant media, blank FeSSIF and blank FaSSIF

Blank FeSSIF and FaSSIF media were prepared as discussed in Section 2.8.1 and were employed to mimic fed and fasted state condition respectively in *in vitro* drug release studies to study the effect of food on release of EA. These media were modified as sodium taurocholate and lecithin can interfere in the analysis and moreover these modified media produces similar results as that by biorelevant media prepared with bile components thus eliminating the addition of sodium taurocholate and lecithin (Zoeller et al., 2007).

#### 3.9.2. In vitro release profile of EA in fed and fasted condition

Release profile of EA from EA suspension and EAPL complex SNEDDS in fed and fasted state is depicted in Fig 13. Release of EA from SNEDDS formulation was higher in both FeSSIF and FaSSIF media (92.18% and 89.75% respectively) with no significant difference between them as compared to that from

EA suspension, where release was much lesser and significantly different in fed and fasted condition. Results demonstrated that the food effect from EA suspension was overcome after the formation of EAPL complex SNEDDS as release from SNEDDS was same in both fed and fasted condition. This unaffected release pattern of EA from EAPL complex SNEDDS may be due to the fact that EAPL complex SNEDDS maintained EA in pre-concentrates and completely solubilized state, which would have formed nanoemulsions of sufficiently small droplet sizes. Moreover, SNEDDS is sufficiently solubilized by itself; therefore dissolution of SNEDDS may have not been dependent on pH condition or ionic concentration. This suggests that avoidance of the lipid dispersion process may have overcome the influence of food on EA release. Thus, EAPL complex loaded SNEDDS would improve patient compliance, particularly in patients not able to take their medicines with food.

### 3.10. Ex vivo permeability studies

Permeability in gastro intestinal tract of any formulation is a crucial factor which decides absorption and bioavailability of drug from that formulation. Hence *ex vivo* permeability studies were carried out to determine permeability of EA in stomach and intestine from SNEDDS and plain drug suspension. The cumulative % permeation of drug from rat stomach and intestine is shown in Fig. 14. It was observed that the permeation of the drug was enhanced from the EAPL complex SNEDDS, in comparison to drug permeation from EA suspension indicating that permeability of drug was increased after formulating SNEDDS. About 84% and 94% of drug was permeated from stomach and intestine respectively in the case of EAPL complex SNEDDS while it was only 23% from stomach and

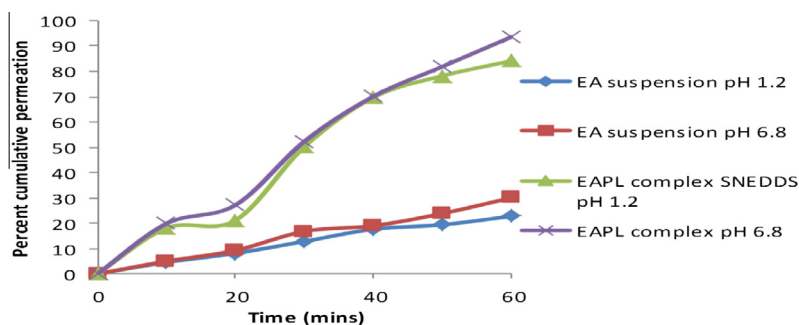


**Figure 14** *Ex-vivo* drug permeation profiles of EAPL complex SNEDDS and EA suspension from rat stomach and intestine.



30% from intestine in the case of EA suspension. It can be noted that permeation of the drug from the intestine was enhanced with SNEDDS, which fulfilled our objective of increasing intestinal permeability for enhancing the bioavailability of EA. Enhanced permeability of EA from SNEDDS can be attributed to absorption mechanism of oil droplet of SNEDDS such as passive diffusion, pinocytosis or endocytosis and their nanometric droplet size providing a large interfacial surface area for drug release and permeation.

#### 4. Conclusion

The present study has undoubtedly proved the potential effectiveness of SNEDDS for formulating EA with improved release profile and permeability. The formulated and optimized EAPL complex SNEDDS composed of EAPL complex (3%), captex (40%), cremophor RH 40 (40%), PEG 400 (20%) and tocopherol (0.15%) was robust to dilution in distilled water at different folds of dilution indicating robustness to dilution and also showed mean globular size, cloud point and zeta potential within the acceptable range. Drug was found to be stable in lipid system in the presence of tocopherol while, EAPL complex prepared by anti-solvent served dual advantages of increasing drug loading as well as solubility. *In vitro* dissolution and *ex vivo* permeability studies revealed improved release profile and permeation of EA, respectively from EAPL complex SNEDDS compared to EA suspension. Moreover, EAPL complex SNEDDS overcame food effect on release pattern of EA. The current investigation may serve as a promising approach for the formulation development of other drugs or phytoconstituents which have limited solubility in both, water as well as lipids.

#### Conflict of interest

There are none.

#### References

- Bell, C., Hawthorne, S., 2008. EA, pomegranate and prostate cancer – A mini review. *J. Pharm. Pharmacol.* 60, 139–144.
- Bala, I., Bhardwaj, V., Hariharan, S., Kumar, M.N.V.R., 2006. Analytical methods for assay of EA and its solubility studies. *J. Pharm. Biomed. Anal.* 40, 206–210.
- Barnaby, S.N., Fath, K.R., Tsiola, A., Banerjee, I.A., 2012. Fabrication of EA incorporated self-assembled peptide microtubes and their applications. *Colloids Surf., B* 95, 154–161.
- Carballo, C.M., Lim, S., Rodriguez, G., Vilac, A.O., Krueger, C.G., Gunasekaran, S., Reed, J.D., 2010. Biopolymer coating of soybean lecithin liposomes via layer-by-layer self-assembly as novel delivery system for EA. *J. Funct. Foods* 2, 99–106.
- Cao, F., Gao, Y., Yin, Z., Ping, Q., 2012. Enhanced oral bioavailability of oleanolic acid in rats with PL complex. *Lett. Drug Des. Discov.* 9, 505–512.
- Chen, M.-L., 2008. Lipid excipients and delivery systems for pharmaceutical development: a regulatory perspective. *Adv. Drug Delivery Rev.* 60, 768–777.
- Craig, D.Q.M., Baker, S.A., Banning, D., Booth, S.W., 1995. An investigation into the mechanisms of self-emulsification using particle size analysis and low frequency dielectric spectroscopy. *Int. J. Pharm.* 11, 103–110.
- Constantinides, P.P., Scalart, J.P., 1997. Formulation and physical characterization of water-in-oil microemulsions containing long-versus medium-chain glycerides. *Int. J. Pharm.* 158, 57–68.
- Constantinides, P.P., 1995. Lipid microemulsions for improving drug dissolution and oral absorption: physical and biopharmaceutical aspects. *Pharm. Res.* 12, 1561–1572.
- Date, A.A., Nagarsenker, M.S., 2007. Design and evaluation of self-nanoemulsifying drug delivery systems (SNEDDS) for cefpodoxime proxetil. *Int. J. Pharm.* 329, 166–172.
- Elnaggar, Y.S.R., El-Massik, M.A., Abdallah, O.Y., 2009. Self-nanoemulsifying drug delivery systems of tamoxifen citrate: design and optimization. *Int. J. Pharm.* 380, 133–141.
- Festa, F., Aglitti, T., Duranti, G., Ricordy, R., Perticone, P., Cozzi, R., 2001. Strong antioxidant activity of EA in mammalian cells in vitro revealed by the comet assay. *Anticancer Res.* 21 (6A), 3903–3908.
- Gershanik, T., Benita, S., 1996. Positively charged self-emulsifying oil formulation for improving oral bioavailability of progesterone. *Pharm. Dev. Technol.* 1, 147–157.
- Gershanik, T., Benita, S., 2005. Self-dispersing lipid formulations for improving oral absorption of lipophilic drugs. *Eur. J. Pharm. Biopharm.* 50, 179–188.
- Gupta, S., Chavhan, S., Sawant, K.K., 2011. Self-nanoemulsifying drug delivery system for adefovir dipivoxil: design, characterization, in vitro and ex vivo evaluation. *Colloids Surf., A* 392, 145–155.
- Häkkinen, S.H., Kärenlampi, S.O., Mykkänen, H.M., Heinonen, I.M., Törrönen, A.R., 2000. EA content in berries: influence of domestic processing and storage. *Eur. Food Res. Technol.* 212, 75–80.
- Hong, J.Y., Kim, J.K., Song, Y.K., Park, J.S., Kim, C.K., 2006. A new self-emulsifying formulation of itraconazole with improved dissolution and oral absorption. *J. Controlled Release* 110, 332–338.
- Hu, Z., Tawa, R., Konishi, T., Shibata, N., Takada, K., 2001. A novel emulsifier, Labrasol, enhances gastrointestinal absorption of gentamicin. *Life Sci.* 69, 2899–2910.
- Itoh, K., Tozuka, Y., Oguchi, T., Yamamoto, K., 2002. Improvement of physicochemical properties of N-4472 part I formulation design by using self-microemulsifying system. *Int. J. Pharm.* 238, 153–160.
- Khan, J., Alexander, A., Saraf, S., Saraf, S., 2013. Recent advances and future prospects of phyto-PL complexation technique for improving pharmacokinetic profile of plant actives. *J. Controlled Release* 168, 50–60.
- Kuntal, M., Kakali, M., Arunava, G., Bishnu, P., Saha, P., Mukherjee, K., 2007. Curcumin-PL complex: preparation, therapeutic evaluation and pharmacokinetic study in rats. *Int. J. Pharm.* 330, 155–163.
- Kommuru, T.R., Gurley, B., Khan, M.A., Reddy, I.K., 2001. Self-emulsifying drug delivery systems (SEDDS) of coenzyme Q10: formulation development and bioavailability assessment. *Int. J. Pharm.* 212, 233–246.
- Landete, J.M., 2011. *Ellagitannins*, EA and their derived metabolites: a review about source, metabolism, functions and health. *Food Res. Int.* 44, 1150–1160.
- Li, B., Harich, K., Wegiel, L., Taylor, L.S., Edgar, K.J., 2013. Stability and solubility enhancement of EA in cellulose ester solid dispersions. *Carbohydr. Polym.* 92, 1443–1450.
- Larrosa, M., García-Conesa, M.T., Espín, J.C., Tomás-Barberán, F.A., 2010. Ellagitannins, EA and vascular health. *Mol. Aspects Med.* 31, 513–539.
- Lei, F., Xing, D.M., Xiang, L., Zhao, Y.N., Wang, W., Zhang, L.J., Dub, L.J., 2003. Pharmacokinetic study of EA in rat after oral administration of pomegranate leaf extract. *J. Chromatogr. B* 796, 189–194.
- Malcolmson, C., Sidhu, A., Satra, C., Kantaria, S., Lawrence, M.J., 1998. Effect of the nature of oil on the incorporation of testosterone propionate into non-ionic oil-in-water microemulsions. *J. Pharm. Sci.* 87, 109–116.
- Mou, D., Chen, H., Du, D., Mao, C., Wan, J., Xu, H., Yang, X., 2008. Hydrogel-thickened nanoemulsion system for topical delivery of lipophilic drugs. *Int. J. Pharm.* 353, 270–276.

- Porat, Y., Abramowitz, A., Gazit, E., 2006. Inhibition of amyloid fibril formation by polyphenols: Structural similarity and aromatic interactions as a common inhibition mechanism. *Chem. Boil. Drug Des.* 67, 27–37.
- Porter, C.J.H., Pouton, C.W., Cuine, J.F., Charman, W.N., 2008. Enhancing intestinal drug solubilization using lipid-based delivery systems. *Adv. Drug Delivery Rev.* 60, 673–691.
- Pathan, R., Bhandari, U., 2011. Preparation characterization of embelin PL complex as effective drug delivery tool. *J. Inclusion Phenom. Macrocyclic Chem.* 69, 139–147.
- Pouton, C.W., Porter, C.J.H., 2008. Formulation of lipid-based delivery systems for oral administration: materials, methods and strategies. *Adv. Drug Delivery Rev.* 60, 625–637.
- Pouton, C.W., 1997. Formulation of self-emulsifying drug delivery systems. *Adv. Drug Delivery Rev.* 25, 47–58.
- Pouton, C.W., 2000. Lipid formulations for oral administration of drugs: non-emulsifying, self-emulsifying and ‘self-microemulsifying’ drug delivery systems. *Eur. J. Pharm. Sci.* 11, S93–S98.
- Pouton, C.W., 2006. Formulation of poorly water-soluble drugs for oral administration: physicochemical and physiological issues and the lipid formulation classification system. *Eur. J. Pharm. Sci.* 29, 278–287.
- Reiss, H., 1975. Entropy-induced dispersion of bulk liquids. *J. Colloid Interface Sci.* 53, 61–70.
- Seeram, N.P., Lee, R., Heber, D., 2004. Bioavailability of EA in human plasma after consumption of *ellagitannins* from pomegranate (*Punicagranatum* L.) juice. *Clin. Chim. Acta* 348, 63–68.
- Sharma, G., Italia, J.L., Sonaje, K., Tikoo, K., Ravi Kumar, M.N.V., 2007. Biodegradable in situ gelling system for subcutaneous administration of EA and EA loaded nanoparticles: evaluation of their antioxidant potential against cyclosporine induced nephrotoxicity in rats. *J. Controlled Release* 118, 27–37.
- Singh, S.K., Verma, P.R.P., Razdan, B., 2010. Development and characterization of a lovastatin loaded self-microemulsifying drug delivery system. *Pharm. Dev. Technol.* 15, 469–483.
- Setthacheewakul, S., Mahattanadul, S., Phadoongsombut, N., Pichayakorn, W., Wiwattanapateee, R., 2010. Development and evaluation of self-microemulsifying liquid and pellet formulations of curcumin, and absorption studies in rats. *Eur. J. Pharm. Biopharm.* 76, 475–485.
- Shyam, K.R., Mruthunjaya, K., Kumar, G.M., 2012. Preparation, characterization and antioxidant activities of gallic acid PLs complex. *Int. J. Res. Pharm. Sci.* 2, 138–148.
- Singh, D., Rawat, M.S.M., Semalty, A., Semalty, M., 2012. Emodin–PL complex. *J. Therm. Anal. Calorim.* 108, 289–298.
- Semalty, A., Semalty, M., Singh, D., Rawat, M.S.M., 2010. Preparation and characterization of PL complexes of naringenin for effective drug delivery. *J. Inclusion Phenom. Macrocyclic Chem.* 67, 253–260.
- Solon, S., Lopes, L., Teixeira de Sousa, P., Schmeda-Hirschmann Jr., G., 2000. Free radical scavenging activity of Lafoensiapacari. *J. Ethnopharmacol.* 72 (1-2), 173–178.
- Shah, N.H., Carvajal, M.T., Patel, C.I., Infeld, M.H., Malick, A.W., 1994. Self-emulsifying drug delivery systems (SEDDS) with polyglycolized glycerides for improving in vitro dissolution and oral absorption of lipophilic drugs. *Int. J. Pharm.* 106, 15–23.
- Shafiq, S., Shakeel, F., Talegaonkar, S., Ahmad, F.J., Khar, R.K., Ali, M., 2007. Development and bioavailability assessment of ramipril nanoemulsion formulation. *Eur. J. Pharm. Biopharm.* 66, 227–243.
- Vattem, D.A., Shetty, K., 2005. Biological functionality of EA: a review. *J. Food Biochem.* 29, 234–266.
- Villar, A.M.S., Naveros, B.C., Campmany, A.C.C., Trenchs, M.A., Rocabert, C.B., Bellowa, L.H., 2012. Design and optimization of self-nanoemulsifying drug delivery systems (SNEDDS) for enhanced dissolution of gemfibrozil. *Int. J. Pharm.* 431, 161–175.
- Venkatesh, M., Maiti, K., Mukherjee, K., Mukherjee, P.K., 2009. Enhanced oral bioavailability and antioxidant profile of ellagic acid by phospholipids. *J. Agric. Food Chem.* 57, 4559–4565.
- Warisnoicharoen, W., Lansley, A.B., Lawrence, M.J., 2000. Nonionic oil-in water microemulsions: the effect of oil type on phase behavior. *Int. J. Pharm.* 198, 7–27.
- Wang, N., Wang, Z.Y., Mo, S.L., Loo, T., Wang, D.M., Luo, H.B., 2012. EA, a phenolic compound, exerts anti-angiogenesis effects via VEGFR-2 signaling pathway in breast cancer. *Breast Cancer Res. Treat.* 134, 943–955.
- Zhang, J., Peng, Q., Shi, S., Zhang, Q., Sun, X., Gong, T., Zhang, Z., 2011. Preparation, characterization, and in vivo evaluation of a self nanoemulsifying drug delivery system loaded with morin-PL complex. *Int. J. Nanomed.* 6, 3405–3414.
- Zhang, P., Liu, Y., Feng, N., Xu, J., 2008. Preparation and evaluation of self microemulsifying drug delivery system of oridonin. *Int. J. Pharm.* 355, 269–276.
- Zoeller, T., Klein, S., 2007. Simplified biorelevant media for screening dissolution performance of poorly soluble drugs. *Dissolution Technol.* 14 (4), 8–13.